Chapter 6

Microstructure and Mechanical Properties of Porous Alumina Fabricated using Rice Husk and Sucrose

6.1. Introduction

This chapter is basically devoted to the study of microstructure of the developed porous alumina ceramics. Also, various mechanical properties such as flexural strength, compressive strength, elastic modulus and hardness of the developed porous alumina have been reported. Microstructure-mechanical property co-relation of samples has been studied to elucidate the effect of porosity and pore size on the corresponding mechanical properties of the developed porous alumina.

6.2. Sample Preparation and Characterization

The procedure for sample preparation to fabricate dry pressed compacts using rice husk and sucrose has already been discussed in the previous chapter.

6.2.1. Porosity and Pore Size Distribution

The total porosity and open porosity of the sintered samples was determined by water immersion method based on Archimedes' principle, using the following Eqn.:[114]

$$\rho = \frac{m_{dry} \times \rho_{water}}{m_{wet} - m_{suspended} + m_{wire}} \quad \text{.....(6.1)}$$

$$\mathrm{P_{total}} = (1 - \frac{\rho}{\rho_{theoretical}}) \times 100 \quad \text{……..(6.2)}$$

$$\mathrm{P_{open}} = \frac{m_{wet} - m_{dry}}{m_{wet} - m_{suspended} + m_{wire}} \times 100 \quad \text{……...(6.3)}$$

where m_{dry} is the dry mass (in g) of the sample, $m_{suspended}$ is the mass of the sample suspended in water, m_{wet} is the mass of the sample after soaking in water, m_{wire} is the mass of the suspending system, ρ_{water} is the density (g/cc) of water, $\mathrm{P_{total}}$ is volume fraction of total porosity of the sample and $\mathrm{P_{open}}$ is volume fraction of

open porosity of the sample. The theoretical density of 3.96 g/cc for fully dense Al_2O_3[63] was used as a reference to calculate volume fraction of total porosity, (Eqn. 6.1, 6.2). The pore size distribution in the samples was also evaluated using mercury porosimetry analyzer, poremaster, PR-33-13 (Quanta chrome instruments, Germany). It can be mentioned here that the lower limit of pore size is 6 nm for porosimetry measurement.

6.2.2. Microstructure

In order to characterize the microstructure of porous alumina samples, fractured samples were positioned in the sample holder using carbon tape and then the sample holder was kept under high vacuum (80 Pa) chamber of the Scanning Electron Microscope (SEM, FEI Inspect S50, Sweden). SEM micrographs give information about pore size, pore shape and pore connectivity. The average pore size was determined using line intercept method from the SEM images using image analysis software (Image Tool, Version 3.0, University of Texas Health Science Center, San Antonio) in the four randomly selected locations on each sample and then calculating the fraction of the pores with size in a certain range.[125]

6.2.3. Mechanical properties

The flexural strength measurements of sintered porous alumina was carried out under three-point bending test using 50 mm x 15 mm x 15 mm samples at a cross head rate of 0.5 mm/min. A screw driven universal testing machine (AGS-5KNND, P/N 340-33309, Shimadzu Corporation Japan) with a maximum load capacity of 10 KN was used for strength testing of sintered porous alumina.[126] Compressive strength was measured in the same UTM machine using samples of 25 mm x 25 mm x 25 mm dimensions at a crosshead rate of 0.5 mm/min. The loaded surfaces were covered with a thin sponge layer to obtain uniform load distribution throughout the faces. The cross-sectional area and the maximum mechanical load were used to calculate the compressive strength of samples. The elastic modulus of porous alumina samples was measured using a dynamic elastic properties analyzer (DEPA, Jagdish Electronics, Bangalore,India) which uses an impulse excitation technique (IET). The samples were excited mechanically by a tapping device. The vibration signal generated by excitation of the samples was analyzed using fast

Fourier transformation (FFT). The measured elastic modulus values were based on the resonant frequency of the samples.[127] Hardness of samples was measured in a hardness tester (Hi-tech India Equipment Pvt. Ltd, India). An average of five samples was used to obtain the average strength, elastic modulus and hardness for each composition.

6.3. Results and Discussion

6.3.1. Porosity and microstructure

Since porosity and pore structure are crucial factors in determining various properties of porous materials, the volume fraction porosity and the corresponding pore size of sintered porous alumina samples were determined as a function of composition such as RH content and its particle size independently. The porosity was characterized quantitatively by determining the values of total and open porosities of porous alumina samples.

A. Effect of RH content

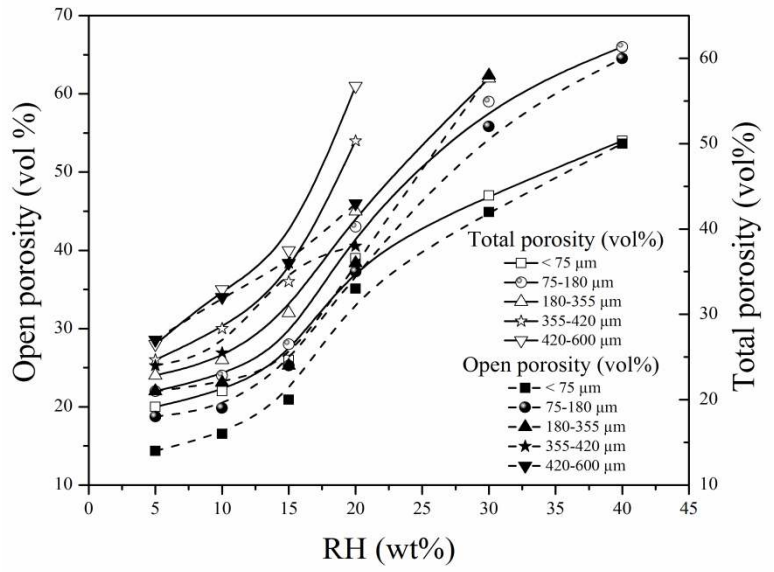

Fig. 6.1 Effect of RH content for various sizes of RH powder on porosity of porous alumina compacts

Fig. 6.1 shows the variation of open porosity and total porosity of developed samples with the volume fraction of RH pore former having different size of RH particles. In all the cases, the lowest total porosity of 20 vol% and maximum total

porosity of 66 vol% was obtained for samples with compositions Al_$^{<75}$RH$_{05}$_SS$_{20}$ and Al_$^{75\text{-}180}$RH$_{40}$_SS$_{20}$, respectively. This porosity is contributed by coarse elongated pores (isolated and/or interconnected) and fine pores. These pores remained in the structure as a result of burning out of RH and sucrose respectively.

Both total and open porosity increased linearly with increasing volume fraction of RH pore former (Fig. 6.1, Table 6.1). Furthermore, Fig. 6.1 shows that the difference between total and open porosities generally decreases as the volume fraction of RH increases. It indicates that the number of interconnected pores increases with increasing volume fraction of RH. The above observation is supported by the microstructures of the samples shown in Fig. 6.2 (a)-(d). These micrographs show an increase in volume fraction of porosity and extent of pore interconnection with increasing addition of RH content for a specific RH size of 75-180 µm. It is quite obvious that the added pore formers are mostly converted into pores after sintering and the pore volume was proportional to the total volume of RH particles. It is important to note that the measured porosity is contributed by a mixture of two types of pores such as elongated large pores and small pores which remained in the structure as a result of burning out of RH and sucrose, respectively. Presence of fine pores, which resulted from sucrose burnout and located in the surrounding region of elongated large pores was confirmed from the micrograph of the samples (Fig. 6.3) taken from the dense region close to an elongated pore of a typical sample composition.

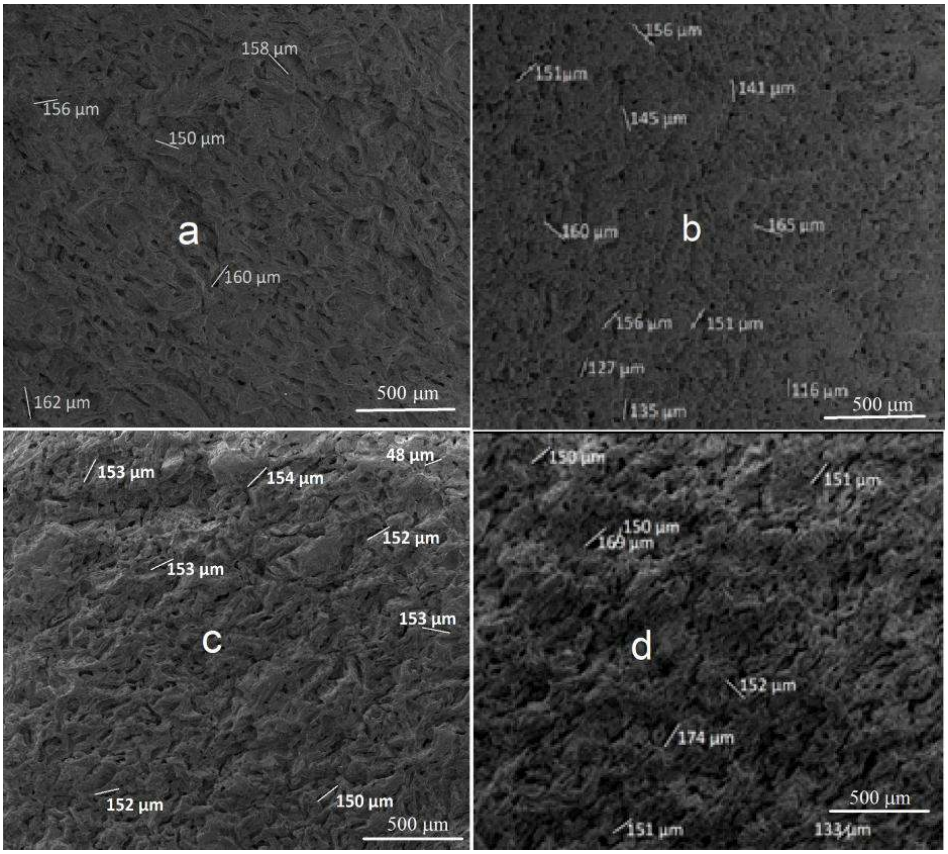

Fig. 6.2 SEM micrograph of sintered porous alumina compacts fabricated using (a) 10, (b) 20, (c) 30 and (d) 40 wt% RH (75-180 µm average size) powder.

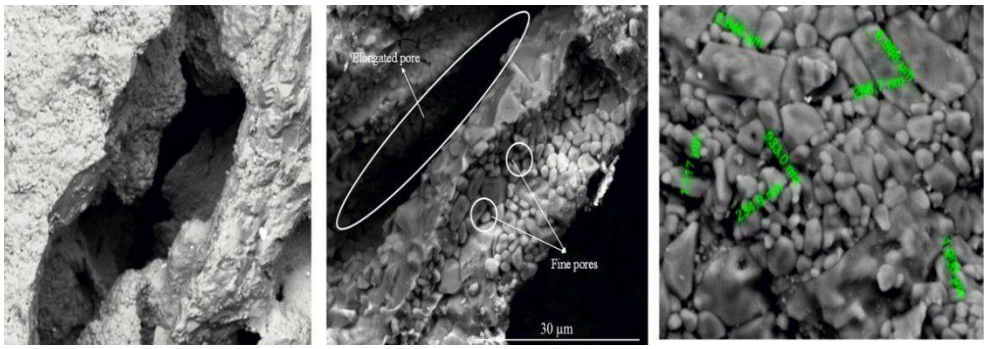

Fig. 6.3 SEM micrograph of a porous alumina compacts showing large elongated pores and fine pores

Table 6.1 Different mixture compositions, the corresponding total porosity, open porosity, average pore size from SEM, interconnection of fabricated porous alumina samples

$Al\_^{x}RH_{y}\_SS_{20}$		% Porosity		Average pore size from SEM (µm)	*Isolated/interconnected
RH content (wt %)	RH powder size (µm)	Total	open		
5	< 75	20	14	50	Isolated
	75-180	22	18.2	140	Isolated
	180-355	24	21.2	295	Isolated
	355-420	26	24	350	Isolated
	420-600	28	27	400	Isolated + interconnected
10	< 75	22	16	52	Isolated
	75-180	24	19	145	Isolated + interconnected
	180-355	26	20.34	300	Isolated + interconnected
	355-420	30	25.2	341	Isolated + interconnected
	420-600	35	32	440	Isolated + interconnected
15	< 75	26	20	60.3	interconnected
	75-180	28	24	156	interconnected
	180-355	32	26	310	interconnected
	355-420	36	28.2	460	interconnected
	420-600	40	36	510	interconnected
20	< 75	39	33	64	interconnected
	75-180	43	35	165.7	interconnected
	180-355	45	36	320.5	interconnected
	355-420	54	38	480	interconnected
	420-600	61	43.61	516	interconnected
30	< 75	47	40.27	66	interconnected
	75-180	59	48.55	175	interconnected
	180-355	62	54.75	340	interconnected
40	< 75	54	46.55	68	interconnected
	75-180	66	60.22	180	interconnected

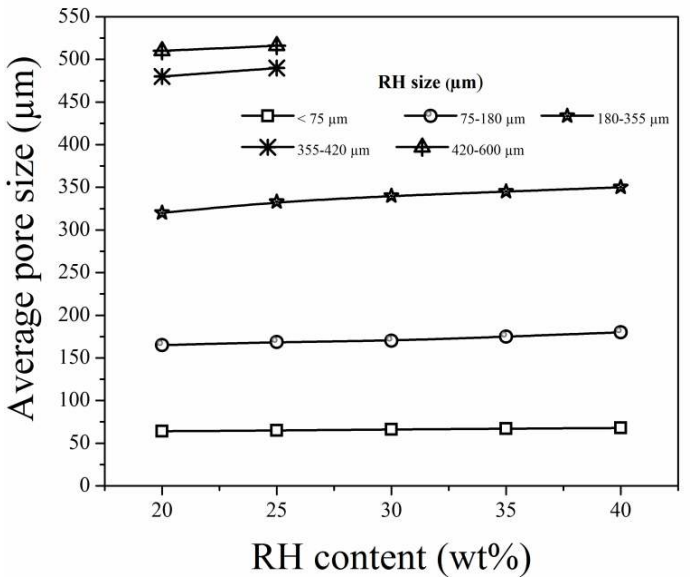

Fig. 6.4 Effect of RH content on average pore size of porous alumina compacts.

Fig. 6.4 also indicates that the pore size increases with increasing volume fraction of RH. This is clearly noted from the microstructures shown in Fig. 6.5 (a)-(e) for the sample with 20 wt% RH of different size of RH. It is noted from Fig. 6.4, that increase in the volume fraction of RH of a fixed size resulted in an increase in pore size of the sintered compacts. This is because the number of interconnected pores increases with increasing volume fraction of RH, (Fig. 6.2 (a)-(d) and Table 6.1). It is interesting to note that, samples containing 5 wt% RH (i.e, Al_$^{<75}$RH$_{05}$_SS$_{20}$, Al_$^{75\text{-}180}$RH$_{05}$_SS$_{20}$, Al_$^{180\text{-}355}$RH$_{05}$_SS$_{20}$, Al_$^{355\text{-}420}$RH$_{05}$_SS$_{20}$, and Al_$^{420\text{-}600}$RH$_{05}$_SS$_{20}$) possess isolated pores only while all the remaining samples contain either partially or fully interconnected pores.

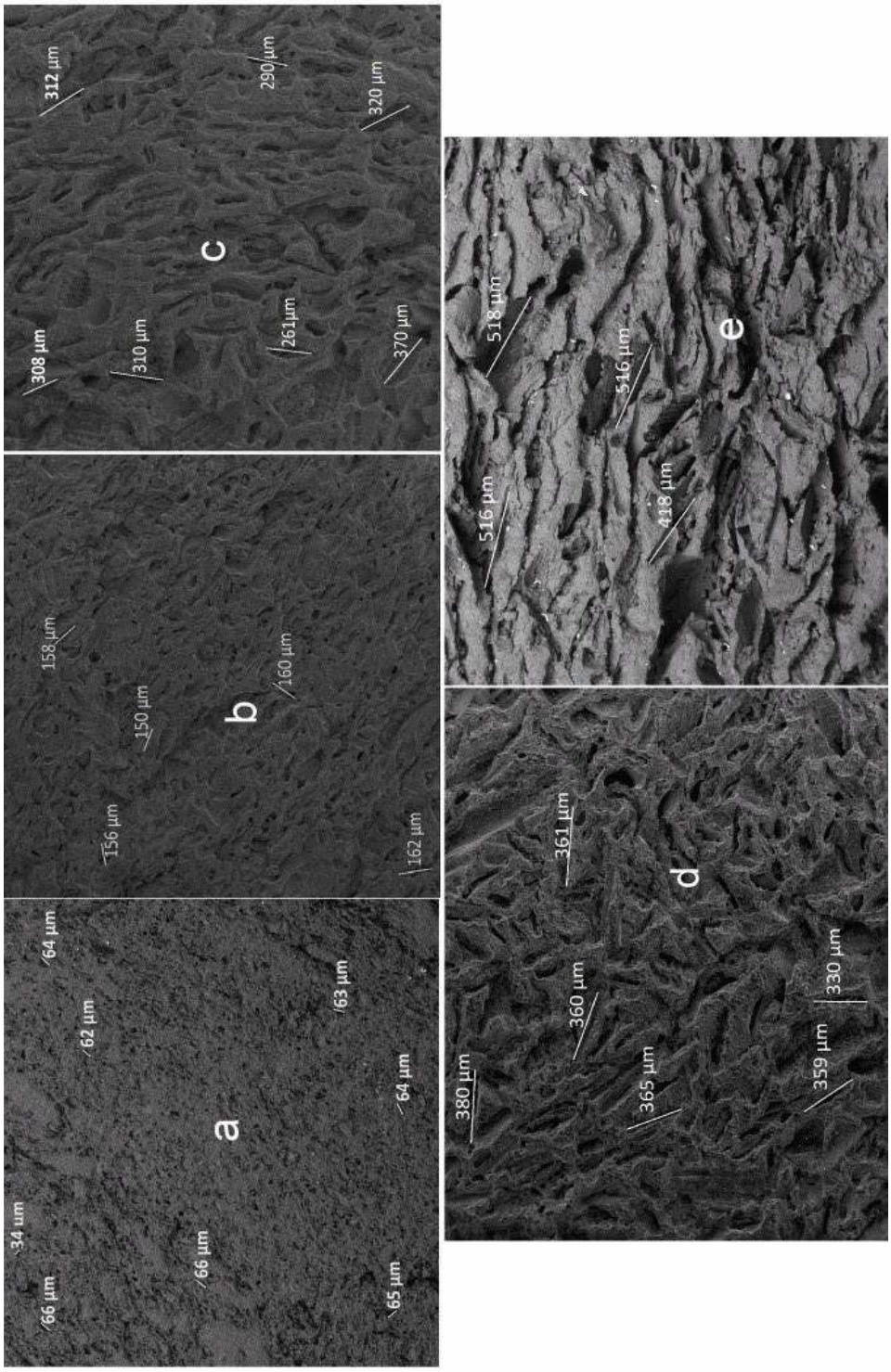

Fig. 6.5 SEM micrograph of sintered porous alumina compacts fabricated using 20 wt% RH powder with (a) <75,(b) 75-180,(c) 180-355, (d) 355-420 and (e) 420-600 µm size

B. Effect of RH size

As shown in Fig. 6.1 that when the size of the pore former increases for a fixed volume fraction of RH, the total porosity of samples increases. The authors believe that the explanation for the above can be linked to two reasons: first, samples prepared from relatively coarser RH powder possess comparatively low green density (Table 5.2) than those prepared with finer RH powder and secondly large pores created during burning out of coarse RH particles undergo less shrinkage in comparison to fine pores (Table 5.3), thus resulting in overall increase in porosity in the sintered compact.[81]

Similarly, variation in avg. pore size of porous alumina with increase in particle size of RH for different volume fraction of RH is shown in (Fig. 6.4). As expected, the average pore size (length) of samples increases from 50 to 516 µm with increasing particle size of RH pore former from <75 to 420-600 µm. It is important to note that, though increase in pore size of porous compacts was observed with increase in RH particle size, the pore size is proportionately less than the original size of RH for each composition due to associated firing shrinkage (Table 5.3). Pores with avg. size in the range 50-516 µm (Table 6.1) were obtained and shrunk linearly by about 11.9-18.3 % (Table 5.3) from the original size of RH. This observation is clear from the sample microstructures shown in Fig. 6.5 (a)-(e), for samples corresponding to 20 wt% RH of sizes <75, 75-180 µm, 180-355 µm, 355-420 and 420-600 µm. Also, the degree of pore interconnection increased with increase in size of RH powder for a fixed amount of RH content in the composition (Fig. 6.5). A minimum porosity of 20 vol%, minimum avg. pore size (length) of 50 µm was measured for sample with initial composition Al_$^{<75}$RH$_{05}$_SS$_{20.}$ On the other hand sample Al_$^{75\text{-}180}$RH$_{40}$_SS$_{20}$ exhibited maximum porosity of 66 vol% and sample Al_$^{420\text{-}600}$RH$_{20}$_SS$_{20}$ showed maximum avg. pore size, among all compositions considered in the present study.

Fig. 6.6 (a) and (b) reveals pore size distributions of typical samples prepared from compositions Al_$^{<75}$RH$_{20}$_SS$_{20}$ and Al_$^{75\text{-}180}$RH$_{20}$_SS$_{20}$. These confirm the presence of coarse as well as fine pores. Fig. 6.6 (a) shows fine pores with avg. size in the range 1-5 µm dia. and elongated coarse pores having size 6-20

μm (dia.). Fig. 6.6 (b) shows fine pores with avg. size 1-5 μm and elongated coarse pores with size 6-20 μm (dia.). These two pore size distribution figures reveal that volume fraction of coarse pores increases with volume fraction and particle size of RH powder. Volume fraction of fine pores decreases with increase in porosity because, these fine pores are trapped within the coarse pores.

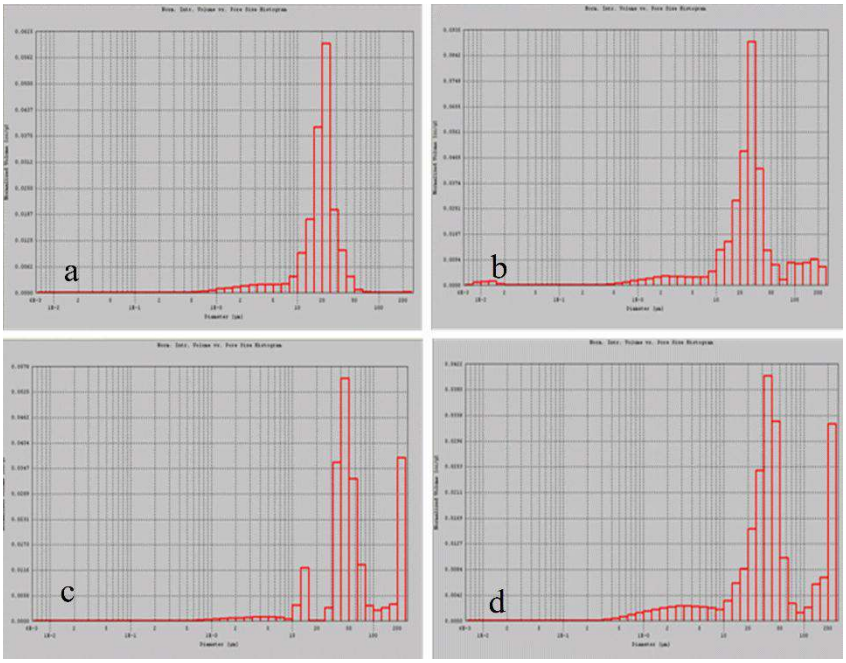

Fig. 6.6 Normalized vol (cc/g) histogram in μm for samples with compositions (a) Al_$^{75\text{-}180}$RH$_{10}$_SS$_{20}$ (b) Al_$^{75\text{-}180}$RH$_{20}$_SS$_{20}$ (c) Al_$^{75\text{-}180}$RH$_{30}$_SS$_{20}$ and (d) Al_$^{75\text{-}180}$RH$_{40}$_SS$_{20}$

SEM micrographs for all compositions confirms the presence of two types of pores viz. large elongated pores with average size 50-516 μm and fine pores with avg. size 4 μm. These results suggest that volume fraction and size of RH can be used to tailor the porosity, pore size and pore connectivity in porous alumina ceramics studied in the present work.

6.3.2. Mechanical properties

Generally, the strength of a porous ceramics is strongly affected by the porosity and pore microstructure. The effect of volume fraction porosity and pore size on strength of porous alumina samples was studied by measuring the flexural strength and compressive strength as a function of porosity and pore size. Strength of each sample was calculated from the maximum of stress at which the sample was

broken. Fig. 6.7 (a) shows the relationship between volume fraction porosity and flexural strength of developed porous alumina samples. For comparison, flexural strength of 380 MPa of a dense alumina sample prepared using this process (reference sample) has been considered.

The flexural strength of porous alumina samples with total porosity of 20-66 vol% was in the range 22.3-207.6 MPa. The sample porosity increased proportionately with increase in volume fraction of RH and its particle size while the flexural strength decreased. This can be understood because porosity and mechanical properties usually are inversely related. Many attempts have been reported to represent the relationship between porosity (P) and fracture strength (σ). The following general Eqn. was proposed by Coble and Kingery,[128] Knudsen[1]

$$\sigma = \sigma_0 exp(-\beta P) \quad \text{.....(6.4)}$$

where P is the volume fraction porosity, σ_0 and β are the fracture strength at P= 0 and an empirical constant obtained from the slope of semi log plot, respectively. The calculated values of σ_0 and β of the developed porous alumina are listed in Table 6.2. The σ_0 and β values of RH based porous alumina samples are compared with those prepared by partial sintering methods by other researchers (Table 6.2).[130-132] It can be seen that the σ_0 (492) value of the developed samples is either comparable or even better than those prepared by various partial sintering methods (73-574). Similarly, the β value (3.1) of RH based porous alumina is lower than that of other samples reported in the literature.[130] The reported β values ranged from 4.0 to 8.3, being slightly higher than the porous samples considered in the present work. Thus, decrease in strength with increase in porosity is less sharp for RH based porous alumina in comparison to other samples.

According to the above formula, strength decreases exponentially with porosity. The strength vs. porosity curve (Fig. 6.7 (a)) also follows the exponential type of trend. The composition Al_$^{<75}$RH $_{05}$_SS$_{20}$ having the lowest total porosity of 20 vol%, exhibited highest flexural strength of 207.6 MPa (Weibull modulus of 10.5). Similarly, lowest flexural strength of 22.3 MPa (Weibull modulus 8.7) was

measured for the sample with compositions Al_$^{75\text{-}180}$RH$_{40}$_SS$_{20}$, which exhibited maximum total porosity of 66 vol%.

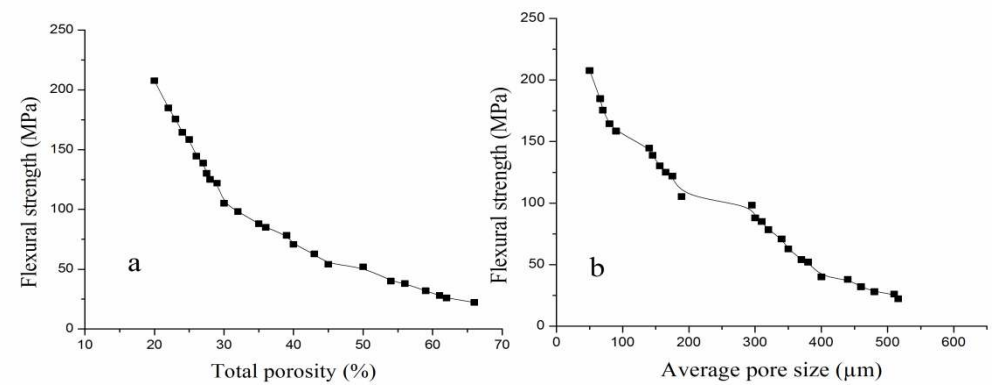

Fig. 6.7 Effect of (a) porosity and (b) pore size on flexural strength of porous alumina compacts.

Table 6.2 Comparison of σ_o and β values of porous alumina ceramics fabricated through different processes.

	Fabrication type	σ_o	β
RH based porous alumina	Organic burn out and sintering	492	3.1
Isobe	Partial sintering	380	4
Spriggs and Vasilos	Partial sintering	73-574	6-8.3
Trostel	Partial sintering	x	5.1

Highest flexural strength of the sample with composition Al_$^{<75}$RH$_{05}$_SS$_{20}$ is attributed to isolated pore microstructure while that with composition Al_$^{75\text{-}180}$RH$_{40}$_SS$_{20,}$ having the lowest flexural strength, possesses interconnected pore microstructure. The strength values are comparable or even much higher than those reported in the literature.[133] The high strength of the porous alumina fabricated in this study can be attributed to not only the full densification of pore walls without any defects but also due to presence of mullite in the alumina matrix which formed during sintering.

The lowering of strength of samples is not only related to increase in porosity but also depends on pore size. Fig. 6.7 (b) shows variation in flexural strength of porous alumina samples as a function of pore size. The strength of

samples decreased with increasing pore size. A relationship between pore size (d) and flexural strength (σ_f) can be expressed by the following Eqn.[130]

$$\sigma_f \alpha \frac{1}{\sqrt{d}} \quad \text{.....(6.5)}$$

With increasing RH size in the composition, the average pore size of the samples increased. This resulted in decrease in flexural strength inversely with square root of pore diameter. The sample with composition Al_$^{<75}$RH$_{05}$_SS$_{20}$ having the smallest pore size (avg. 50 µm) exhibited highest flexural strength of 207.6 MPa. In contrast, the sample Al_$^{420\text{-}600}$RH$_{20}$_SS$_{20}$, which shows maximum pore size of 516 µm. did not exhibit minimum strength. Rather, lowest strength of 22.3 MPa was achieved for the sample Al_$^{75\text{-}180}$RH$_{40}$_SS$_{20}$ (corresponding to maximum porosity), which exhibited an intermediate value of avg. pore size of 180 µm. This observation concludes that, both porosity and pore size combinely affect the strength of porous ceramics.

To summarize, samples with flexural strength in the range 22.3 to 207.6 MPa have been obtained in this process. Zhang et al. have reported values of 3-point bending strength of a typical porous alumina sample having 34.51 % porosity with an average 165 µm pore length and 132 µm pore dia. equal to 155±20 MPa.[63] In comparison, flexural strength of our samples with 35 % porosity is 98 MPa. Slightly lower strength in our samples may be due to presence of randomly oriented interconnected pores.

Similar to flexural strength, the compressive strength of samples increased remarkably from 9.18 to 180 MPa by decreasing the porosity from 66 to 20 vol% and pore size from 516 to 50 µm, as shown in Fig. 6.8 (a) and (b).

These strength values are comparable or even much higher than those reported in the literature.[42] The high compressive strength of the porous ceramics fabricated in this work is attributed not only to full densification of pore walls (RH-originated pores) without any defects, but also due to the presence of mullite in the alumina matrix that formed during sintering. The sample Al_$^{<75}$RH$_{05}$_SS$_{20}$ having the lowest total porosity of 20 vol% and pore size of 50 µm, exhibited highest

compressive strength of 180 MPa. On the other hand, a minimum compressive strength of 9.18 MPa was achieved for the sample Al_$^{75\text{-}180}$RH$_{40}$_SS$_{20}$ (corresponding to maximum porosity of 66 vol%).

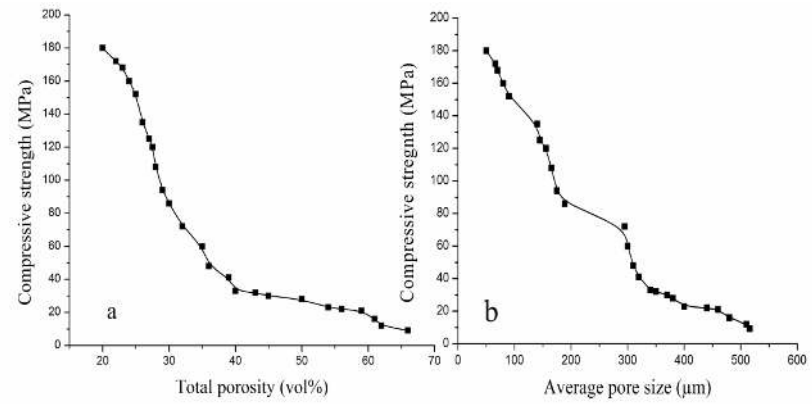

Fig. 6.8 Effect of (a) porosity and (b) pore size on compressive strength of porous alumina compacts.

The elastic modulus of fully dense alumina samples fabricated using this process is 380 GPa. The elastic modulus of porous alumina samples plotted as function of porosity is given in Fig. 6.9 (a). The following general Eqn. was proposed by Knudsen[129] and Spriggs[131] for the dependence of elastic modulus on porosity.

$$E = E_0 exp(-\beta P) \quad \text{.....(6.6)}$$

where E is the elastic modulus of a fully dense alumina, P is the porosity and β is an empirical constant. Variation of elastic modulus with porosity agreed well with the above model.

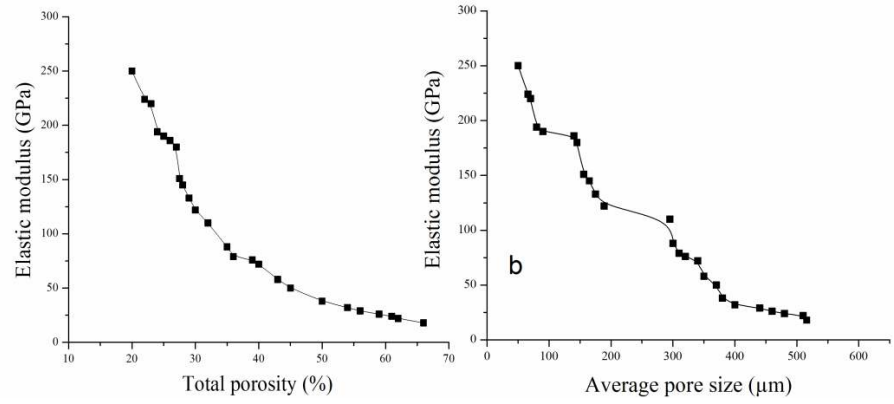

Fig. 6.9 Effect of (a) porosity and (b) pore size on elastic modulus of porous alumina compacts.

The results shown here suggest that the increasing porosity within the range of 20 to 66 vol% causes a rapid decrease in elastic modulus exponentially from 250 GPa to 18 GPa. It is interesting to note that for porosity greater than a critical value (50 vol%), the change is almost negligible. Similarly, elastic moduli of samples with pore size in the range 50 to 516 µm were in the range 250-18 GPa., composition Al_$^{<75}$RH$_{05}$_SS$_{20}$ having the highest modulus and sample Al_$^{75-180}$RH$_{40}$_SS$_{20}$ having the lowest elastic modulus (Fig. 6.9 (b)).

Hardness of porous alumina samples decreased to a value of 18 HRD as the total porosity increased to 66 vol%, as shown in Fig. 6.10 (a). The hardness value drops dramatically with increasing porosity till a critical pore content (50 vol%), beyond which, it decreased less rapidly. The hardness of porous alumina samples was also investigated as a function of pore size. Fig. 6.10 (b) clearly shows that the hardness decreases with increasing pore size of the samples. Hardness of samples with porosity 20-66% and pore size in the range 50 to 516 µm was in the range 149-18 HRD, sample with composition Al_$^{<75}$RH$_{05}$_SS$_{20}$ having the highest and sample Al_$^{75-180}$RH$_{40}$_SS$_{20}$ having lowest hardness.

In a recent review of the influence of the porosity on physical properties, Rice reported the significance of percolation limit, P_c (critical porosity limit), which is a value of P (volume fraction porosity) above which a specific physical

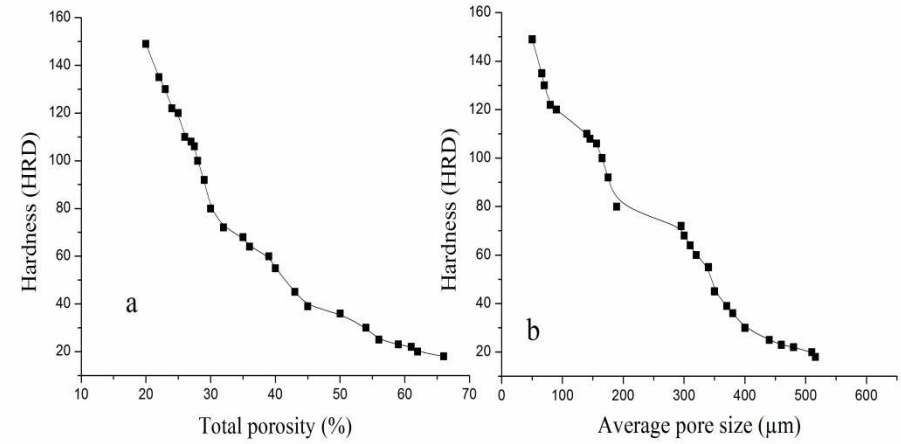

Fig. 6.10 Effect of (a) porosity and (b) pore size on hardness of porous alumina samples

property (e.g, elastic modulus, hardness, strength etc.) is insensitive to further changes in porosity or relative density.[134] In this work our results agree well with

the above theory. The percolation limit of porosity in our case is approximately 50 vol% and the limit corresponding to pore size is approximately 400 µm beyond which the properties are almost independent of porosity and pore size. At $P>P_c$, the particle–particle contact is insufficient to fully transmit the physical forces. In other words, minimum SAF (Solid Area Fraction) strongly influences the physical properties of porous materials. It has been observed that all the mechanical properties studied here show a single percolation limit and it is suggested that these are controlled by particle-particle cross-sectional contact area.

6.4. Summary

1. In summary, the present work reported the microstruatural analysis and mechanical properties of the developed porous alumina ceramics.
2. Porous alumina ceramics with isolated and/or interconnected pores with porosity in the range 20-66 vol% were successfully fabricated using this process.
3. SEM micrographs of porous alumina ceramics showed mixture of two types of pores such as randomly oriented elongated coarse pores with avg. size (length) in the range 50-516 µm and fine pores with avg. size 4 µm created during burnout of RH and sucrose, respectively.
4. The mechanical properties of developed porous alumina samples decreased exponentially with increase in porosity and pore size till a percolation limit (50 vol% porosity and 400 µm pore size), beyond which the effect of microstructure on properties was negligible.
5. The flexural strength, compressive strength, elastic modulus, and hardness value of the obtained porous alumina ceramics were in the range 207.6 to 22.3 MPa, 180 to 9.18 MPa, 250 to 18 GPa and 149 to 18 HRD, respectively.